J. Fluid Mech. (1976), *vol.* 74, *part* 4, *pp.* 641–665
Printed in Great Britain

The locking-on of vortex shedding due to the cross-stream vibration of circular cylinders in uniform and shear flows

By P. K. STANSBY

Atkins Research and Development, Ashley Road, Epsom, Surrey, England†

(Received 22 May 1974 and in revised form 18 August 1975)

The frequencies of vortex shedding from circular cylinders forced to oscillate transversely in low-turbulence uniform and shear flows were investigated. The stream velocity in the shear flow varied linearly with spanwise distance.

In both flows the vortex shedding frequency locked on to the cylinder frequency and to submultiples of the cylinder frequency. In uniform flow the range of cylinder frequencies for locking-on was dependent on the amplitude of oscillation and Reynolds number. At the boundaries of locking-on at the cylinder frequency locked-on shedding was intermittent with unforced shedding and locking-on was accompanied by a change in wake width. At a particular cylinder frequency near mid-range it is conjectured that the wake width jumped from being greater to being less than that for the stationary cylinder. In shear flow the spanwise extent of locking-on at the cylinder frequency was explained by considering the uniform flow results and the inclination of shed vortices in shear flow. At the spanwise boundaries of this locking-on, locked-on cells were shed intermittently with unforced cells which were more stable in frequency than the corresponding cells for the stationary cylinder.

1. Introduction

1.1. *Uniform flow*

For a bluff cylinder spanning a uniform stream, the Kármán vortex street occurs in its purest form at Reynolds numbers of a few hundred. At higher Reynolds numbers the wake is complicated by the presence of turbulence, but it is known from experiments that periodic vortex shedding occurs in some form at all Reynolds numbers from about 100 up to at least 8×10^6.

Because of the presence of the vortex street, a bluff cylinder in a stream experiences a fluctuating lift, with a strong component at the frequency n_s at which pairs of vortices are shed. Hence the flow past a cylinder may cause the cylinder to oscillate transversely, especially if the cylinder's natural frequency is close to the shedding frequency.

If n_{s0} is the vortex shedding frequency for a stationary cylinder in a stream, vibrations of the cylinder at a frequency n_c which is close to n_{s0} may cause vortex

† Present address: Department of Civil Engineering, University of Salford, Salford M5 4WT, England.

shedding at the frequency n_c. This 'locking-on' of the vortex shedding to the cylinder frequency can occur over a range of flow speeds dependent on the amplitude of cylinder vibration a and Reynolds number Re. Locking-on causes the vortex shedding to be almost perfectly correlated across the span, which in turn causes the amplitude of vibration to increase. Thus experiments in which a cylinder is spring-mounted, but not driven mechanically, are difficult to interpret. Hence, to investigate the relationship between the vortex shedding frequency n_s, the cylinder's oscillation frequency n_c and the amplitude of oscillation a, it is better to drive the cylinder mechanically.

Some of the first experiments of this kind were made by Bishop & Hassan (1964), who investigated the lift on a circular cylinder oscillating in a flow of water. They found that, in the locked-on range, at a certain value of n_c/n_{s0} there were jumps in the amplitude of the lift and in the phase of the lift relative to the cylinder displacement. This value of n_c/n_{s0} was dependent on whether the cylinder frequency was decreasing or increasing. They also found that vortex shedding could lock on at a half and a third of the cylinder frequency. (For convenience locking-on at the cylinder frequency, at half the cylinder frequency and at a third of the cylinder frequency will be referred to as primary, secondary and tertiary locking-on respectively.)

Further investigations in air have largely substantiated these findings. In general, however, little attention has been paid to end effects although it has been shown by Stansby (1974) that end effects may have a large influence on the wake structure of circular cylinders with aspect ratios even as large as 20. In the experiments to be described, particular attention has been paid to the removal of end effects. Interest was mainly in the ranges of the different kinds of locking-on and the manner of vortex shedding at their boundaries.

Using the symbols already described, it can be shown that S_s ($= n_s D/U$) is dependent on only S_c ($= n_c D/U$), a/D and Re ($= UD/\nu$), provided there are no end effects, where U is the flow speed, ν the kinematic viscosity and D the diameter of the cylinder.

1.2. *Shear flow*

The flows past many structures such as chimneys or underwater piles are shear flows, generated as boundary layers on the earth in a natural wind or on the bed of the sea or a river. Thus it is important to understand the way in which a vortex wake is formed in shear flow. This has been investigated by Maull & Young (1973) and by Mair & Stansby (1975) for stationary cylinders in a low-turbulence shear flow with the upstream velocity varying almost linearly with spanwise distance. The fluctuating lift can still cause a cylinder to vibrate, and further experiments were made to investigate the relationship between the amplitude of cylinder oscillation, the vortex shedding frequencies across the span, the frequency of cylinder oscillation, and the velocity gradient of the incident flow. Again the cylinder was driven mechanically.

It is worthwhile considering the ways in which the features of vortex wakes of oscillating cylinders in uniform flow and of stationary cylinders in shear flow might interact to produce the vortex wakes in this situation. But first it is neces-

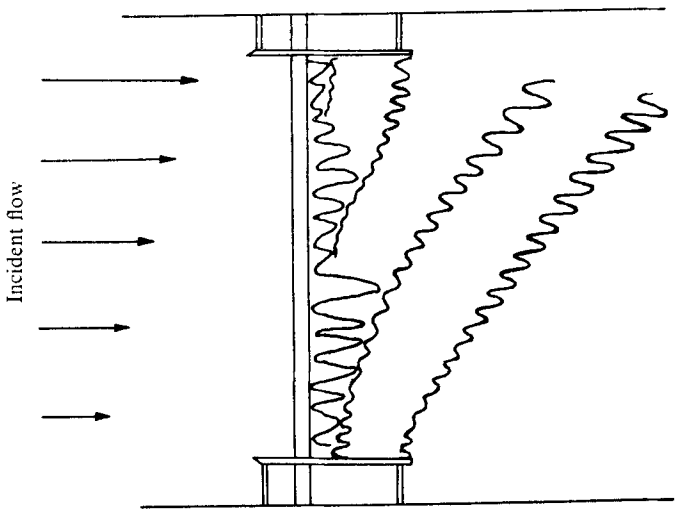

FIGURE 1. Vortex shapes shed from 25·4 mm cylinder when stationary in shear flow, shown by smoke visualization.

sary to outline the prominent characteristics of vortex wakes of stationary cylinders in shear flow.

Vortex shedding from stationary cylinders in shear flow occurs in cells of different frequency and of finite spanwise length. The frequency of shedding in a cell is dependent on the upstream velocity, in that the local Strouhal number (based on the local upstream velocity) tends to vary little across the span of the cylinder. This might be expected from quasi-two-dimensional considerations as the Strouhal number in uniform flow varies little with Reynolds number in the range considered. However, the situation is complicated by end effects, and the local Strouhal number shows greater variation across the whole span than is to be expected from the variation of the upstream velocity across the length of a cell. In some cases a cell of a certain frequency is always shed from the same segment of the span but in others the cell boundaries fluctuate and there is a range of shedding frequencies associated with a given spanwise position. What actually happens is dependent on external conditions, e.g. the end conditions, and each different situation has to be investigated in its own right. A further important consideration is the upstream influence of the downstream vortices. By injecting smoke into the cylinder boundary layer, it is shown in figure 1 (a sketch of one frame of a ciné film) that the shed vortices appear to form lines across the span inclined in sympathy with the incident upstream velocities. (In uniform flow the vortices were inclined at less than 10° to the cylinder axis.) The vorticity in the shear flow should rotate the axis of a shed vortex as it moves downstream, but it can be seen that the vortices close to the body appear to have similar inclinations to the downstream ones (away from the influence of the end plates, which vortices must approach normally); this is possibly because the three-dimensionalities of the downstream wake were being fed upstream to the base of the cylinder.

As there will be a range of values for n_{s0} across a cylinder span in shear flow, when the cylinder is oscillating there will be a corresponding range of values of n_c/n_{s0}. A simple comparison with uniform flow would suggest that locking-on might occur, for a given a/D, for the ranges of n_c/n_{s0} for which it occurs in uniform flow. This might be expected in a quasi-two-dimensional situation except that in shear flow the vortices are inclined to the cylinder axis, imposing three-dimensional effects, and locking-on in uniform flow is essentially a two-dimensional phenomenon. However, locking-on is likely to be an important phenomenon as a locked-on cell will probably have greater spanwise length and coherence at the shedding frequency and also greater vortex strength than the other cells.

2. The importance of aspect ratio in shear flow

The end effects caused by tunnel-wall boundary layers are thought to be eliminated by using end plates of the design specified by Stansby (1974) and similar end plates were used in these experiments in both uniform and shear flows. Thus the frequency of shedding from a circular cylinder oscillating in shear flow will depend on only the following parameters: the kinematic viscosity ν; the velocity gradient of the incident shear flow λ, which in this case is approximately independent of spanwise position; the cylinder diameter D; a representative velocity of the flow, taken to be the velocity at mid-tunnel U_M; the distance between the end plates H; the distance y from the mid-tunnel position to the station considered; the cylinder oscillation frequency n_c; and the amplitude of the oscillation a.

As the flow is incompressible

$$S_s = n_s D/U_M = F(R_M, \beta_M, y/D, H/D, S_c, a/D),$$

where $$R_M = U_M D/\nu, \quad \beta_M = \lambda D/U_M \quad \text{and} \quad S_c = n_c D/U_M.$$

It was shown by Mair & Stansby (1975) that in shear flow the length of the end plates downstream of the body affected the cell formation with the 25·4 mm diameter cylinder with $H/D = 16$. So, for this body, end plates extending $12{\cdot}0D$ downstream of the body were used, in order to give stable cell formation. It was shown that for stationary cylinders, even near the centre of the span, the vortex wake was dependent on H/D when H/D was less than 20. For these experiments, only cylinders of diameter 25·4 and 50·8 mm were used and as the greatest possible value of H was 406 mm, the maximum value of H/D was only 16. For values of R_M of $1{\cdot}3 \times 10^4$ and $2{\cdot}6 \times 10^4$ Mair & Stansby found that for $H/D < 8$ there were only two stable end cells. For $H/D = 16$ there was a region in mid-span extending for about $8D$ which was distinct from the end cells, even though the cell structure was still dependent on the end conditions. At the Reynolds numbers of the present experiments a similar region was found, only with unstable cells (see § 5.1), and these cells were the nearest approach to cells free from end effects for which the effect of cylinder oscillation could be investigated. For reasons described in § 3.3 the upper limit of S_c for the 25·4 mm cylinder was smaller than that for the

50·8 mm cylinder, and secondary and tertiary locking-on could be investigated only with the 50·8 mm cylinder. For this cylinder, at the maximum H/D of 8 there are only the two stable end cells, but it was thought worthwhile to use this cylinder to investigate secondary and tertiary locking-on and also to investigate the effects of a different β_M.

3. Design of experiments

3.1. *Apparatus*

The experiments were performed in an open-return wind tunnel with a working section 508 mm high and 711 mm wide. The turbulence intensity in the uniform free stream (u'/U) was approximately 0·25 %. The cylinders spanned the wind tunnel vertically. Adjustable holes were made in the wind-tunnel floor and ceiling to accommodate the cylinders and their vibration. The cylinders were supported at either end at the mid-points of very thin, spring-steel beams, the ends of which were effectively pin-jointed and supported on a strong tubular frame. This frame did not touch the wind tunnel, so that vibration could not be transmitted from it to the tunnel except through the laboratory floor. To prevent flow through the holes in the tunnel floor and ceiling, very thin sheet rubber was stretched over the end of the cylinder when in position.

The two ends of the cylinder were made to oscillate in phase and with the same amplitude, using a motor driving two eccentrics. To avoid stresses in the oscillating system the natural frequency of the spring-beam/cylinder arrangement could be tuned to the desired oscillation frequency, so all the oscillating forces were concentrated at the spring supports. These could then be neutralized by using tunable vibration absorbers.

Holes were also made in the end plates to accommodate the cylinders and their vibration. Flow through these holes was prevented by using very thin pieces of sheet steel glued to the cylinders and in sliding contact with the inner faces of the end plates. In this way the plane inner surface of an end plate was effectively extended to the cylinder circumference.

To investigate the vortex wake a hot-wire probe was placed outside the turbulent wake, $1{\cdot}00D$ downstream of and $2{\cdot}15D$ across from the centre of the cylinder in its mid-position (unless otherwise stated). The signal, suitably treated, was recorded on a magnetic tape, to be later replayed into an analog-to-digital converter and analysed on a small digital computer. The analysis gave the variation of the power spectral density of the hot-wire signal with frequency and the phase difference ϕ between the component of the hot-wire signal at the cylinder frequency and the cylinder displacement, together with the coherence between these two signals.

The shedding frequency n_s and the cylinder frequency n_c were obtained from the computed curves of power spectral density against frequency. ϕ was computed for each hot-wire signal and it was confirmed that the coherence at n_c was close to unity, thereby ensuring very little error in ϕ.

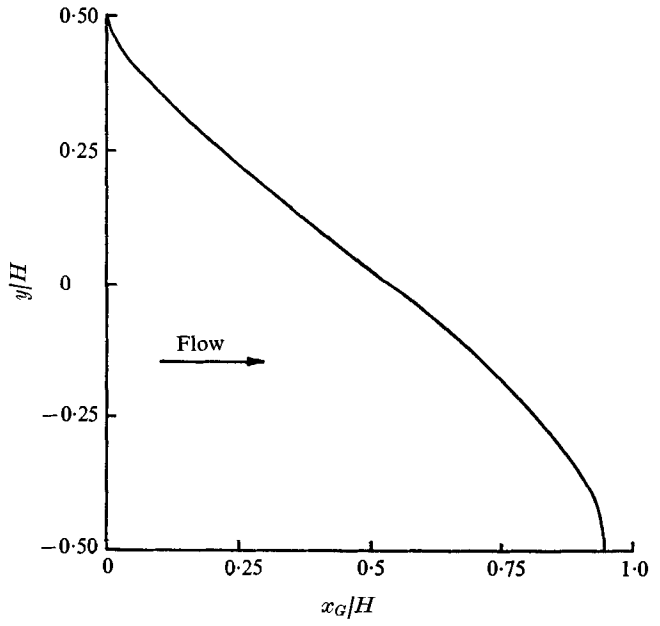

FIGURE 2. Shape of gauze used to generate the shear flow. H = height of working section, x_G = horizontal distance downstream of datum.

3.2. *Shear flow in a wind tunnel*

Various methods have been used for generating a shear flow in a wind tunnel. A number of these have been based on the use of some form of graded resistance, such as the grid of rods suggested by Owen & Zienkiewicz (1957), but a disadvantage of these methods is the turbulence generated in the free stream. For the present work the shear flow was generated by means of a curved sheet of wire gauze, as studied theoretically by Elder (1959) and later developed by Maull (1969). The gauze was shaped as shown in figure 2 and placed near the upstream end of the long working section of the wind tunnel. The measurements were made in a region about 2 m downstream of the central part of the gauze, where the velocity distribution between the end plates described in § 2 without the body in place was as shown in figure 3. This distribution did not change significantly with wind speed, over the range used. Further measurements in the same region showed that the intensity of turbulence (u'/U_M) was about 0·4 %.

The streamlines are deflected upwards by the curved gauze, although further downstream they become nearly parallel again. Measurements of the velocity direction and static pressure in the measurement region showed that the streamlines were straight and parallel to within about 1°.

3.3. *Experimental procedure*

The parameters on which S_s is dependent are described in § 1.1 for uniform flow and in § 2 for shear flow. By the same arguments ϕ, for a given probe position, is dependent on the same parameters for each situation.

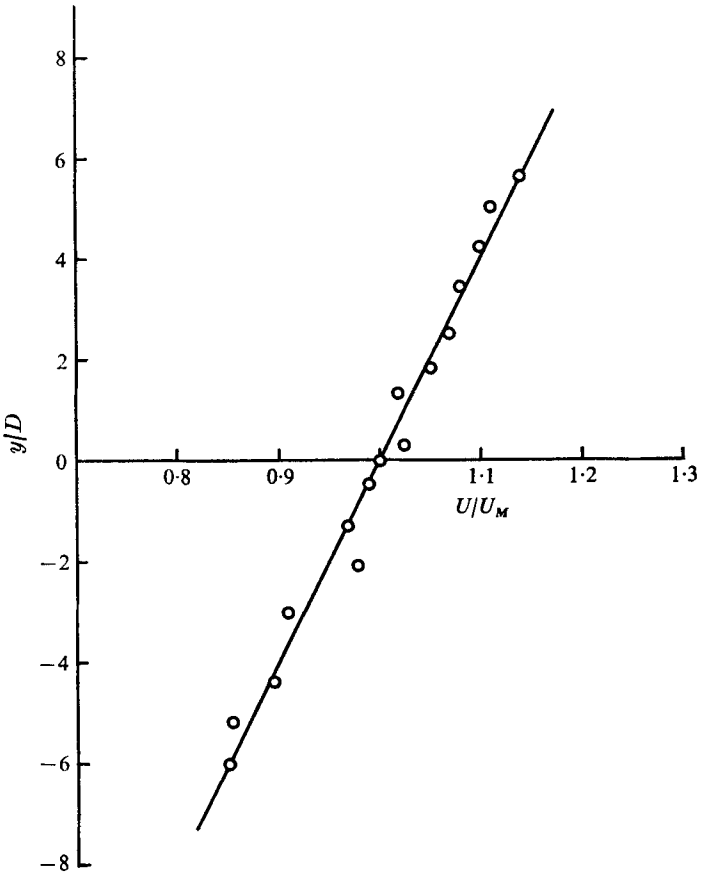

FIGURE 3. Velocity profile between the end plates without the body in position. U = local velocity, D = 25·4 mm.

The range of S_c for a given cylinder is determined by the upst ream inciden velocity (at mid-tunnel in shear flow) and the frequency of cylinder oscillation. The maximum value of the latter was about 22 Hz and the minimum value of the former was defined by practical considerations. As the wind tunnel was of the open-return type, small fluctuations in the air pressure in the laboratory influenced the flow in the working section when the difference between the pressures inside and outside the working section was small. With wind speeds not less than about 2 m/s the flow in the tunnel was found to be reasonably steady.

In uniform flow S_c/S_0 was varied between 0·40 and 3·20 with the 50·8 mm cylinder, the Reynolds number being 9200 for $S_c/S_0 < 2{\cdot}3$ and 7000 for $S_c/S_0 > 2{\cdot}3$. With the 25·4 mm cylinder S_c/S_0 was varied between 0·40 and 1·40 at a Reynolds number of 3600.

In shear flow, values of S_s up to 0·354 were used with the 50·8 mm cylinder, the mid-tunnel Reynolds number being 9100; with the 25·4 mm cylinder, the Reynolds number was 3700 and the largest value of S_c was 0·198. H/D and β_M

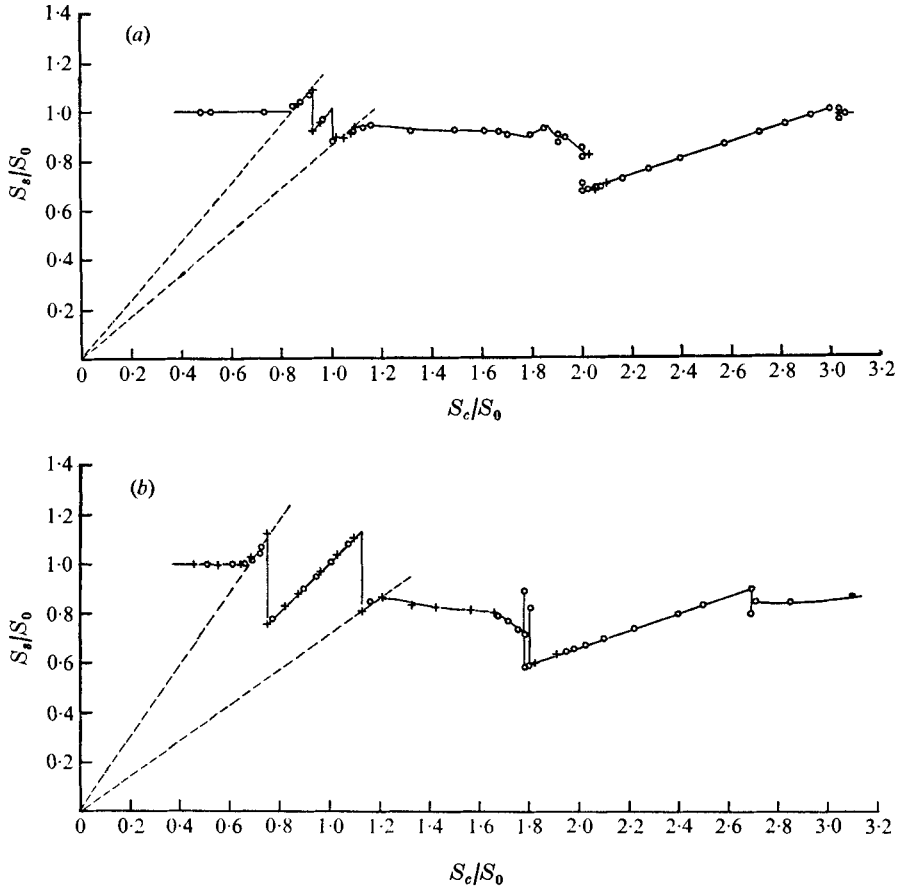

FIGURE 4. The variation of S_s/S_0 with S_c/S_0 in uniform flow with (*a*) $a/D = 0{\cdot}10$ and (*b*) $a/D = 0{\cdot}29$ for $Re \approx 9200$ ($0 < S_c/S_0 < 2{\cdot}3$) and 7000 ($S_c/S_0 > 2{\cdot}3$). ○, increasing cylinder frequency; +, decreasing cylinder frequency.

were determined by the cylinder diameter in these experiments as the magnitudes of H and λ/U_M were virtually fixed.

No attempt was made to correct the experimental results for blockage, although its effect in relation to hysteresis is discussed in §4.2.

4. Uniform flow

4.1. *Results*

Variation of shedding frequency with cylinder frequency. Curves of S_s/S_0 against S_c/S_0 are shown in figures 4 (*a*) and (*b*) for $a/D = 0{\cdot}10$ and $0{\cdot}29$ respectively, with $Re \approx 9200$ for $S_c/S_0 < 2{\cdot}3$ and $Re \approx 7000$ for $S_c/S_0 > 2{\cdot}3$. They show how primary and tertiary locking-on occur for a range of S_c/S_0 dependent on a/D. Secondary locking-on occurs for only a very small range of S_c/S_0 with $a/D = 0{\cdot}10$.

When shedding is not locked-on, S_s/S_0 is unity for cylinder frequencies below the range of primary locking-on. Above this range S_s/S_0 is less than unity by an

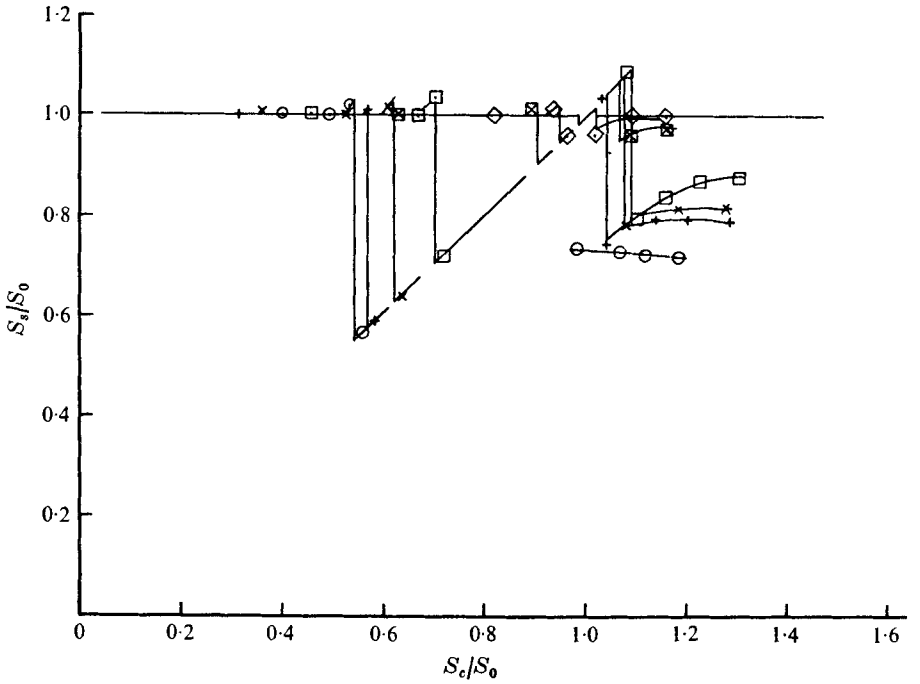

FIGURE 5. The variation of S_s/S_0 with S_c/S_0 in uniform flow with $Re \approx 3600$. —, $a/D = 0{\cdot}01$; ◇, $a/D = 0{\cdot}02$; ⊠, $a/D = 0{\cdot}06$; □, $a/D = 0{\cdot}20$; ×, $a/D = 0{\cdot}30$; +, $a/D = 0{\cdot}38$; ○, $a/D = 0{\cdot}48$.

amount which increases as a/D decreases, and generally decreases slightly as S_c/S_0 increases. The different Reynolds numbers for S_c/S_0 above and below the range of tertiary locking-on could influence the corresponding magnitudes of S_s/S_0. The experiments made at $Re \approx 3600$ confirm these trends (see figure 5).

Secondary locking-on did not occur with $a/D = 0{\cdot}29$ (figure 4 *b*). However, the spectra at the lower limit of tertiary locking-on have broad peaks with frequencies between $\frac{1}{2}n_c$ and $\frac{1}{3}n_c$, shown by the vertical lines in figure 4 (*b*). This means that the frequency was varying with time between these limits.

The boundaries of primary locking-on have two prominent characteristics. There are ranges of cylinder frequency where S_s/S_0 is approximately proportional to S_c/S_0, as shown by the broken lines in figures 4 (*a*) and (*b*). Within these ranges of S_c/S_0, or boundary zones, the oscilloscope trace of the hot-wire signal (for a given cylinder frequency) showed the shedding to change intermittently between being locked-on and not locked-on. The vertical lines in figures 4 (*a*) and (*b*) show where the shedding has become completely locked-on. The experiments made at $Re \approx 3600$ showed similar boundary zones of smaller extent. It is noteworthy that for $a/D = 0{\cdot}48$ there is no upper boundary zone, while there is for $a/D = 0{\cdot}38$.

At the boundaries of tertiary locking-on the behaviour is different. Intermittent locking-on is shown by two peaks in the spectrum, at $\frac{1}{3}n_c$ and at the unlocked-on shedding frequency. This occurs at the lower boundary for $a/D = 0{\cdot}10$, where the power spectrum for $S_c/S_0 = 2{\cdot}01$ (with increasing cylinder frequency) has two broad peaks at $\frac{1}{3}n_c$ and $0{\cdot}40n_c$ (approximately). The

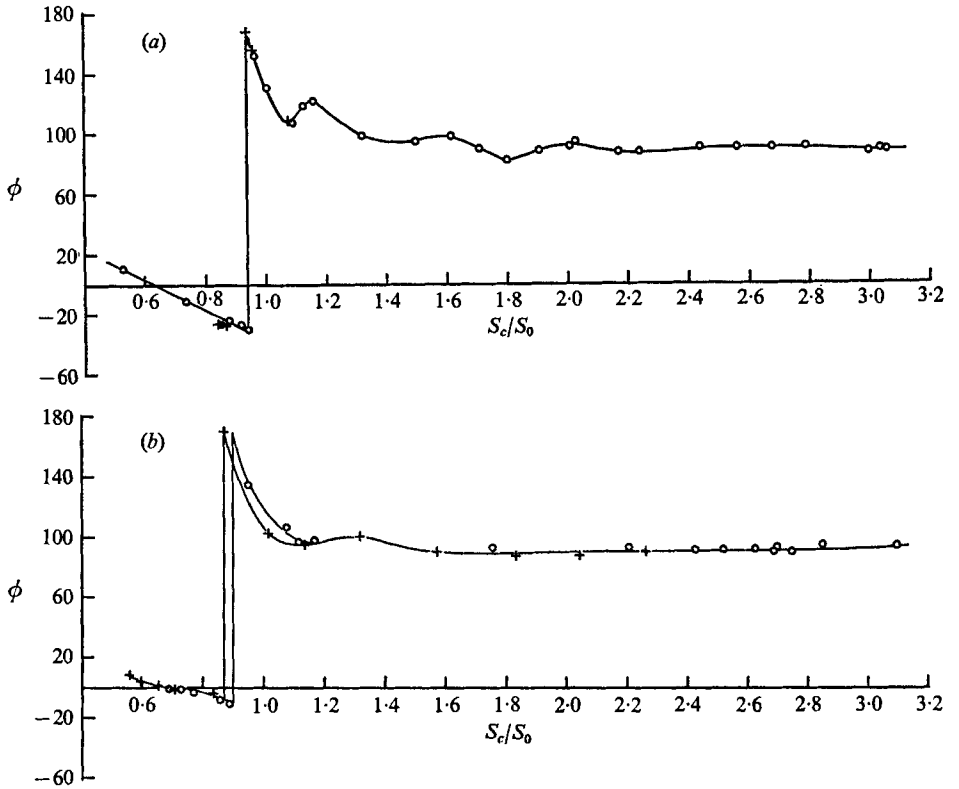

FIGURE 6. The variation of ϕ with S_c/S_0 in uniform flow with (*a*) $a/D = 0{\cdot}10$ and (*b*) $a/D = 0{\cdot}29$ for $Re \approx 9200$ ($0 < S_c/S_0 < 2{\cdot}3$) and 7000 ($S_c/S_0 > 2{\cdot}3$). ○, increasing cylinder frequency; +, decreasing cylinder frequency.

corresponding value of S_c/S_0 for decreasing cylinder frequency was not found precisely but the results show that it must be about 2·03. The lower boundary for $a/D = 0{\cdot}29$ has been described above. At the upper boundaries of locking-on there is no evidence of intermittent locking-on and the spectra have broad peaks with frequencies shown by the vertical lines in figures 4 (*a*) and (*b*). Thus intermittent locking-on occurs only at the lower boundary at a single value of S_c/S_0 which is dependent on whether the cylinder frequency is increasing or decreasing.

Primary locking-on never occurred for $a/D = 0{\cdot}03$ with $Re \approx 9200$ but it did occur for $a/D = 0{\cdot}01$ with $Re \approx 3600$.

Variation of ϕ with cylinder frequency. ϕ is presented as a function of S_c/S_0 in figures 6 (*a*) and (*b*) for $a/D = 0{\cdot}10$ and 0·29 respectively, with $Re \approx 9200$ for $S_c/S_0 < 2{\cdot}3$ and $Re \approx 7000$ for $S_c/S_0 > 2{\cdot}3$. The curves show a jump in ϕ of about 180° at a particular value of S_c/S_0 which is less than 1·00 by an amount which increases as a/D increases. For $a/D = 0{\cdot}10$ there is no discernible hysteresis associated with the jump but for $a/D = 0{\cdot}29$ the values of S_c/S_0 at the jump differ by 0·03 for increasing and decreasing cylinder frequency. Experiments made at $Re \approx 3600$ with the 25·4 mm cylinder showed no hysteresis effects and values of S_c/S_0 at the jump are given in table 1 for a wide range of a/D.

a/D	0·01	0·02	0·06	0·20	0·30	0·38	0·48
Values of S_c/S_0 at the jump in ϕ with $Re \approx 3600$	1·00	0·98	0·96	0·88	0·86	0·84	0·83

TABLE 1

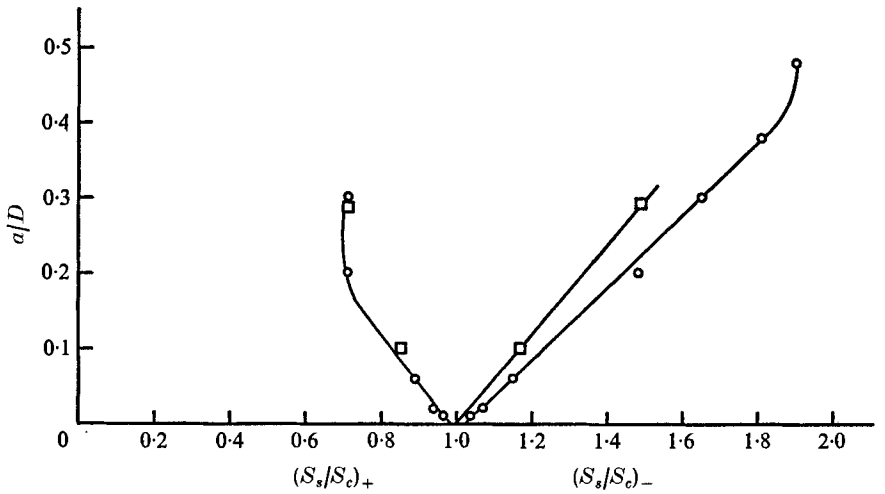

FIGURE 7. The ratios S_s/S_c in the boundary zones of primary locking-on in uniform flow for different a/D. □, $Re \approx 9200$; ○, $Re \approx 3600$.

For cylinder frequencies below the jump, ϕ decreases uniformly with increasing S_c/S_0 and there is no effect due to primary locking-on. For cylinder frequencies above the jump, primary locking-on has a large influence. When there is complete locking-on ϕ decreases rapidly with increasing S_c/S_0 but it varies little for cylinder frequencies above the upper boundary zone, being virtually unaffected by secondary and tertiary locking-on. The upper boundary zones are characterized by ϕ increasing with increasing S_c/S_0. This was not found for $a/D = 0{\cdot}48$ in the experiments made at $Re \approx 3600$, which otherwise showed the same trends.

4.2. *Discussion*

The ranges of locking-on. Figures 4 (*a*) and (*b*) show that S_s/S_0 is approximately proportional to S_c/S_0 in the boundary zones of primary locking-on. In these zones of intermittent shedding it is assumed that the base pressure is the same whether the shedding is locked-on or not. Using the concept of Roshko's universal Strouhal number, described in the appendix, locking-on can be shown to be accompanied by a change in wake width. At the lower limit locking-on causes an increase in wake width and at the upper limit a decrease. The ratio of locked-on wake width to unforced wake width is equal to S_s/S_c ($= n_s/n_c$). These values are plotted against a/D in figure 7, where the suffix minus denotes the lower limit and the suffix plus the upper limit.

The results for the 25·4 mm cylinder at $Re \approx 3600$ are also plotted and at the lower boundaries the equation

$$(S_s/S_c)_- = 1{\cdot}02(1 + 2{\cdot}00a/D)$$

fits these points for $a/D \leqslant 0{\cdot}38$. If the points for $Re \approx 9200$ also lie on a straight line, the equation

$$(S_s/S_c)_- = 1{\cdot}00(1 + 1{\cdot}69a/D)$$

describes the lower limit of locking-on for $0{\cdot}10 \leqslant a/D \leqslant 0{\cdot}29$.

At the upper boundaries the points for both cylinders, i.e. with $Re \approx 3600$ and 9200, lie on a single curve which can be described by

$$(S_s/S_c)_+ = 0{\cdot}99(1 - 1{\cdot}60a/D)$$

for $a/D \leqslant 0{\cdot}06$. For $a/D = 0{\cdot}48$ there is no upper boundary zone, suggesting that locked-on shedding does not occur above the jump in ϕ. The change in wake structure accompanying the jump in ϕ will be discussed below. For $a/D = 0{\cdot}38$ the upper boundary zones does exist and it would appear from figure 7 that the condition

$$(S_s/S_c)_+ = (d'_c/d'_s)_+ \geqslant 0{\cdot}73$$

must be satisfied for locked-on shedding to occur.

The jumps in ϕ of about 180° at certain cylinder frequencies near the middle of the locked-on range suggest a sudden change in the wake structure. If wake width does not change with cylinder frequency when shedding is not locked-on, then $d'_{s-} = d'_{s+} = d'_0$ and $d'_{c+} \neq d'_{c-}$. If d'_c does not change in the locked-on range except at the jump in ϕ then the wake width must change by $d'_{c-} - d'_{c+}$ at the jump in ϕ. These assumptions may not be strictly correct and further experiments would be necessary to verify them. However, they seem likely approximations and they fit together to explain the experimental results at least qualitatively. The hysteresis effects are discussed later in this subsection.

For secondary locking-on there were no jumps in S_s/S_0 and the range of locking-on, when it occurred, was small. In contrast, the ranges of tertiary locking-on were large and there was some evidence of intermittent locking-on at the lower boundaries but not at the upper boundaries. Jumps in S_s/S_0 with intermittent locking-on are indicative of jumps in wake width and thus appear to be symptomatic of locking-on over ranges of cylinder frequency dependent on a/D. For tertiary locking-on there were no jumps in ϕ indicating sudden changes in wake structure.

The result that primary and tertiary but not secondary locking-on occur for ranges of cylinder frequency is worthy of further discussion. The association with wake width leads one to consider the positions of the cylinder in relation to the vortex street. Vortices are shed at intervals of $(2n_s)^{-1}$. At any given instant the cylinder will be in a certain position in relation to the vortex street. At a time $(2n_s)^{-1}$ later the street will be a mirror image of the original situation and, if the cylinder is back in its original position, the wake width will be similar to that for the stationary cylinder. This concurs with the situation for locking-on at even submultiples of the cylinder frequency (e.g. secondary locking-on). However, for

	$a/D = 0{\cdot}10$		$a/D = 0{\cdot}29$	
	Change in δ_1	$\Delta S_c/S_0$	Change in δ_1	$\Delta S_c/S_0$
At the lower limit of primary locking-on	0·006	—	0·018	—
At the jump in ϕ	0·012	—	0·030	0·03
At the upper limit of primary locking-on	0·005	—	0·011	—
At the lower limit of tertiary locking-on	0·007	0·02	0·006	—
At the upper limit of tertiary locking-on	0·007	—	0·006	—

TABLE 2

primary locking-on and locking-on at odd submultiples of the cylinder frequency (e.g. tertiary locking-on), the second cylinder position will, in general, be different from the original position (the maximum separation being $2a$) and will cause the wake width to be different from that for the stationary cylinder.

The experimental results are thus given a qualitative explanation. It should be remembered that the concept of a universal Strouhal number is inherent in this explanation and further research is needed to establish fully its relation to oscillating bodies.

Hysteresis. Hysteresis was detected only for the 50·8 mm cylinder; at the jump in ϕ with $a/D = 0{\cdot}29$, and at the lower limit of tertiary locking-on with $a/D = 0{\cdot}10$. The difference $\Delta S_c/S_0$ in the values of S_c/S_0 for increasing and decreasing cylinder frequencies are given in table 2. That no hysteresis was detectable at the jumps in ϕ for the 25·4 mm cylinder suggests that blockage may be important.

The effect of blockage is to cause the effective free-stream velocity U_c to be greater than U by $U\delta$, so that

$$U_c/U = 1+\delta,$$

where δ can be determined for stationary cylinders by Maskell's (1965) method.

As S_0 does not vary detectably with small changes in U,

$$S_{0\,\mathrm{cor}}/S_0 = 1+\delta,$$

where the suffix cor denotes the corrected value. Therefore

$$S_c/S_0 = (S_c/S_{0\,\mathrm{cor}})\,(1+\delta).$$

Blockage is dependent on wake width and it is suggested earlier in this subsection how this is changed by cylinder oscillation.

If δ_0 and $\delta_0+\delta_1$ refer respectively to stationary and oscillating cylinders then

$$\delta_1/\delta_0 = (d_1'-d_0')/d_0'.$$

If the jumps in the magnitude of d' occur at a certain $S_c/S_{0\,\mathrm{cor}}$, the corresponding values of S_c/S_0 will depend on whether the jump is approached with increasing or decreasing cylinder frequency. By substituting δ_0 and the appropriate values of d_1'/d_0' in the equation above, δ_1 can be determined. The changes in δ_1, which are listed in table 2 for various situations, are seen to correspond to the values of

$\Delta S_c/S_0$ found experimentally ($3\delta_1$ being equivalent to $\Delta S_c/S_0$ at the lower limit of tertiary locking-on), suggesting that hysteresis may be entirely due to blockage.

For the 25·4 mm cylinder, $\delta_0 = 0{\cdot}02$ and the values of $\Delta S_c/S_0$ were presumably too small to be detected experimentally.

The minimum value of a/D for locking-on at the cylinder frequency. At $Re \approx 3600$ there is primary locking-on with $a/D = 0{\cdot}01$ while at $Re \approx 9200$ there is no such locking-on with $a/D = 0{\cdot}03$. The boundary zones for $Re \approx 9200$ are much wider than those for $Re \approx 3600$ and it would appear that locking-on ceases when the inner limits coincide. That there should be such a difference at these two Reynolds numbers can perhaps be explained by the difference in wake structure as indicated by the large change in C_{pb} between the two Reynolds numbers (e.g. see Linke 1931). However, it is possible that the different downstream lengths of the end plates or the different aspect ratios might have influenced the results.

5. Shear flow

5.1. *Experimental results*

The spanwise distribution of shedding frequency for the stationary cylinders. For the 25·4 mm cylinder, with $H/D = 16$, the power spectra for various spanwise positions are shown in figure 8 and the corresponding values of S_s are plotted in figure 9 (*a*) for rather more spanwise positions. At a given height the width of the peak in the spectrum represents the range of shedding frequencies which can occur and the spanwise envelope of the shedding frequencies defines all the possible cell formations, as at any given time each cell has a finite length and a single frequency and cells do not overlap. Over most of the span the spectra do not show the well-defined peaks that occurred at higher Reynolds numbers but there are still two well-defined end cells, although they have variable length. For the 50·8 mm cylinder the spanwise distribution of S_s is shown in figure 9 (*b*) and it can be seen that there are only two end cells, each of variable length.

The spanwise distribution of shedding frequency for different a/D and S_c. As was anticipated earlier the spanwise extent of primary locking-on increases as a/D increases. This is demonstrated by the spanwise distributions of S_s for the 25·4 mm cylinder with $a/D = 0{\cdot}06$ and $S_c = 0{\cdot}198$ (figure 10*a*) and with $a/D = 0{\cdot}20$ and $S_c = 0{\cdot}167$, where the shedding is just locked-on at the cylinder frequency across the whole span. This is further shown by the spanwise distributions of S_s for the 50·8 mm cylinder, where the two-cell wake structure of the stationary cylinder is modified by cylinder oscillation. Figure 10 (*b*) shows for $a/D = 0{\cdot}10$ and $S_c = 0{\cdot}168$ two well-defined end cells with an additional cell locked-on at the cylinder frequency near mid-span, while for $a/D = 0{\cdot}24$ and $S_c = 0{\cdot}176$ the shedding is just locked-on at the cylinder frequency across the whole span. Secondary and tertiary locking-on was found with this cylinder for $a/D = 0{\cdot}29$ and $S_c = 0{\cdot}280$ and $0{\cdot}354$ (figure 11).

A notable feature shown by the spanwise distributions of S_s is the influence of cylinder oscillation on the unforced cells adjacent to the cell locked-on at the cylinder frequency. Power spectra for various spanwise positions are shown in figure 12 for the 25·4 mm cylinder with $a/D = 0{\cdot}06$ and $S_c = 0{\cdot}198$. The unforced

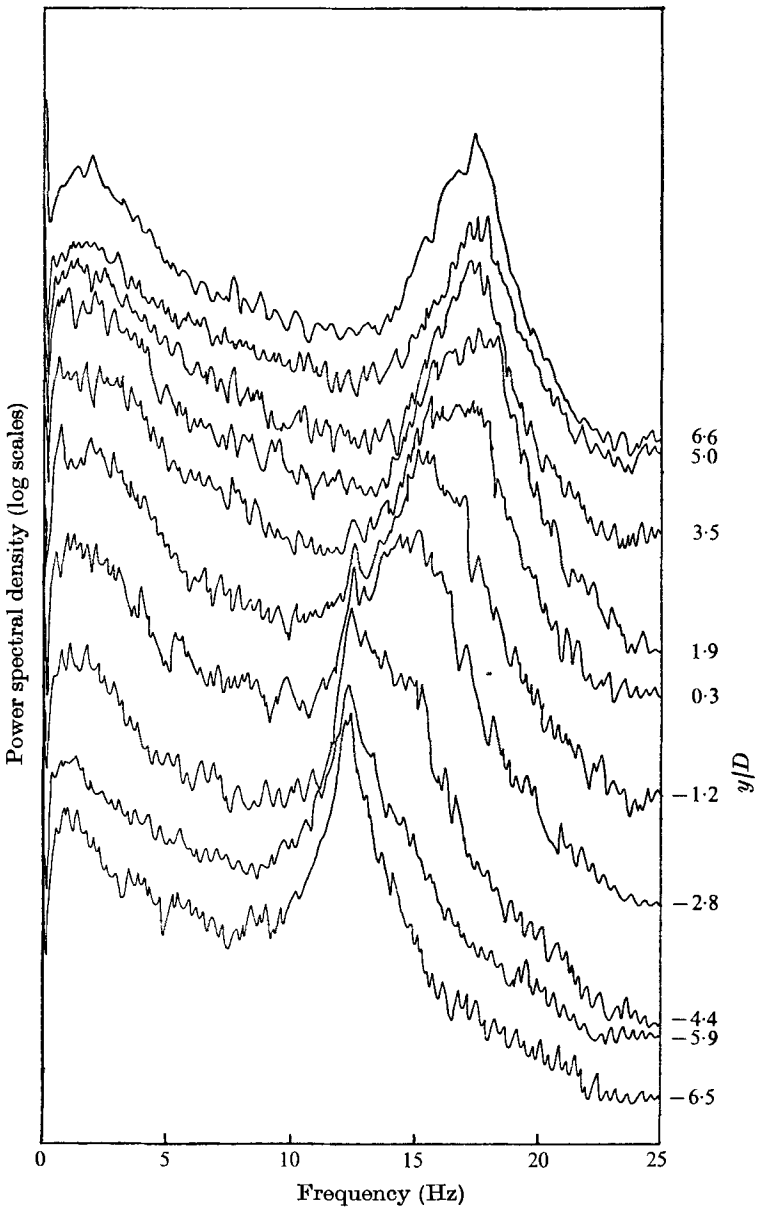

FIGURE 8. Frequency spectra at various spanwise positions for the stationary cylinder with $H/D = 16$.

cells adjacent to the locked-on cells are slightly unsteady in frequency but, relative to the corresponding regions for the stationary cylinder, the ranges of possible shedding frequency are much smaller. The value of S_s for the upper cell (adjacent to the locked-on cell) is greater than that for the upper end cell of the stationary cylinder, while the value of S_s for the lower end cell (not adjacent to the locked-on cell) is the same as for the stationary cylinder. At the same a/D

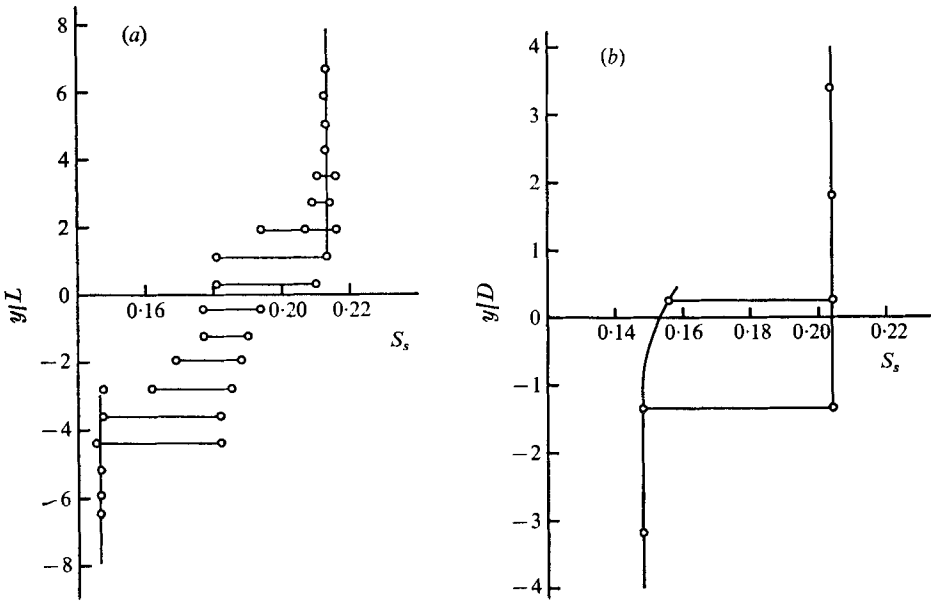

FIGURE 9. Spanwise distribution of S_s for the stationary cylinder with (*a*) $H/D = 16$ and (*b*) $H/D = 8$.

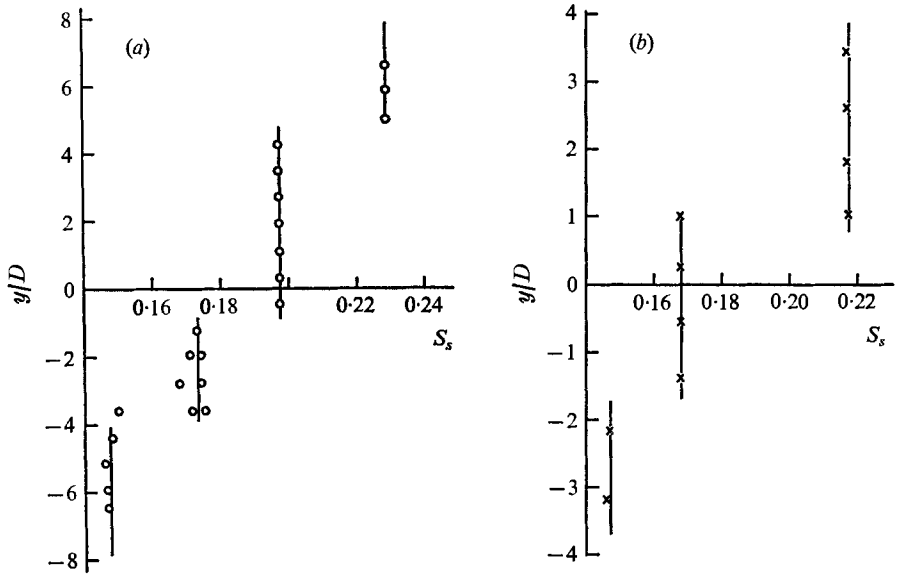

FIGURE 10. Spanwise distributions of S_s with (*a*) $H/D = 16$, $a/D = 0{\cdot}06$ and $S_c = 0{\cdot}198$ and (*b*) $H/D = 8$, $a/D = 0{\cdot}10$ and $S_c = 0{\cdot}168$.

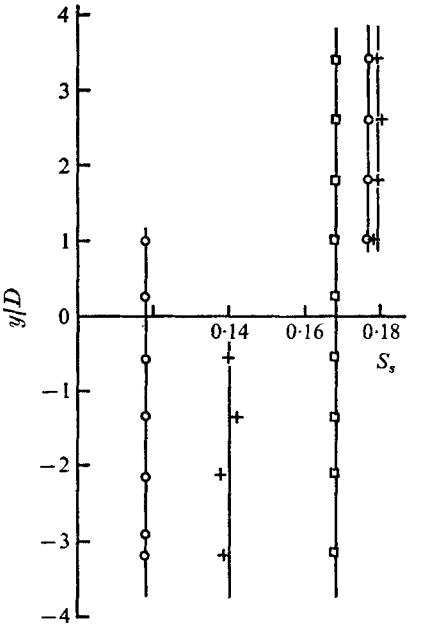

FIGURE 11. Spanwise distributions of S_s with $H/D = 8$ and $a/D = 0{\cdot}29$.
○, $S_c = 0{\cdot}354$; +, $S_c = 0{\cdot}280$; □, $S_c = 0{\cdot}168$.

with $S_c = 0{\cdot}155$, the value of S_s for the lower end cell is forced below the value for the stationary cylinder, while the unforced cell above the locked-on cell has a much smaller range of possible shedding frequencies than the corresponding cells of the stationary cylinder. Table 3 gives the values of S_c for locked-on cells, with the values of S_s for adjacent cells, for different a/D and H/D. When S_c is outside the range of S_s for the stationary cylinder, cylinder oscillation has little 'stabilizing' effect on the cell structure, as shown in figure 13 for the 25·4 mm cylinder with $a/D = 0{\cdot}20$ and $S_c = 0{\cdot}107$. However, the value of S_s for the lower end cell is forced above that for the stationary cylinder and is included in table 3.

A similar table cannot be constructed from the data available for secondary and tertiary locking-on. However, it can be seen how the values of S_s are changed from those for the stationary cylinder.

The spanwise variation of ϕ for different a/D and S_c. When there is no primary locking-on over any part of the span there is very little spanwise variation of ϕ, although its magnitude can vary for different situations. This is exemplified by the spanwise distributions for the 25·4 mm cylinder with $a/D = 0{\cdot}20$ and $S_c = 0{\cdot}107$ (figure 14) and for the 50·8 mm cylinder with $a/D = 0{\cdot}29$ and $S_c = 0{\cdot}280$ and $0{\cdot}354$ (figure 15), although for $S_c = 0{\cdot}280$ there is a small variation in the upper part of the span. When vortex shedding is locked-on at the cylinder frequency across the whole span, the spanwise variation of ϕ is large except in the regions close to the end plates (see figure 14 for the 25·4 mm cylinder with $a/D = 0{\cdot}20$ and $S_c = 0{\cdot}167$ and figure 15 for the 50·8 mm cylinder with $a/D = 0{\cdot}29$ and $S_c = 0{\cdot}168$).

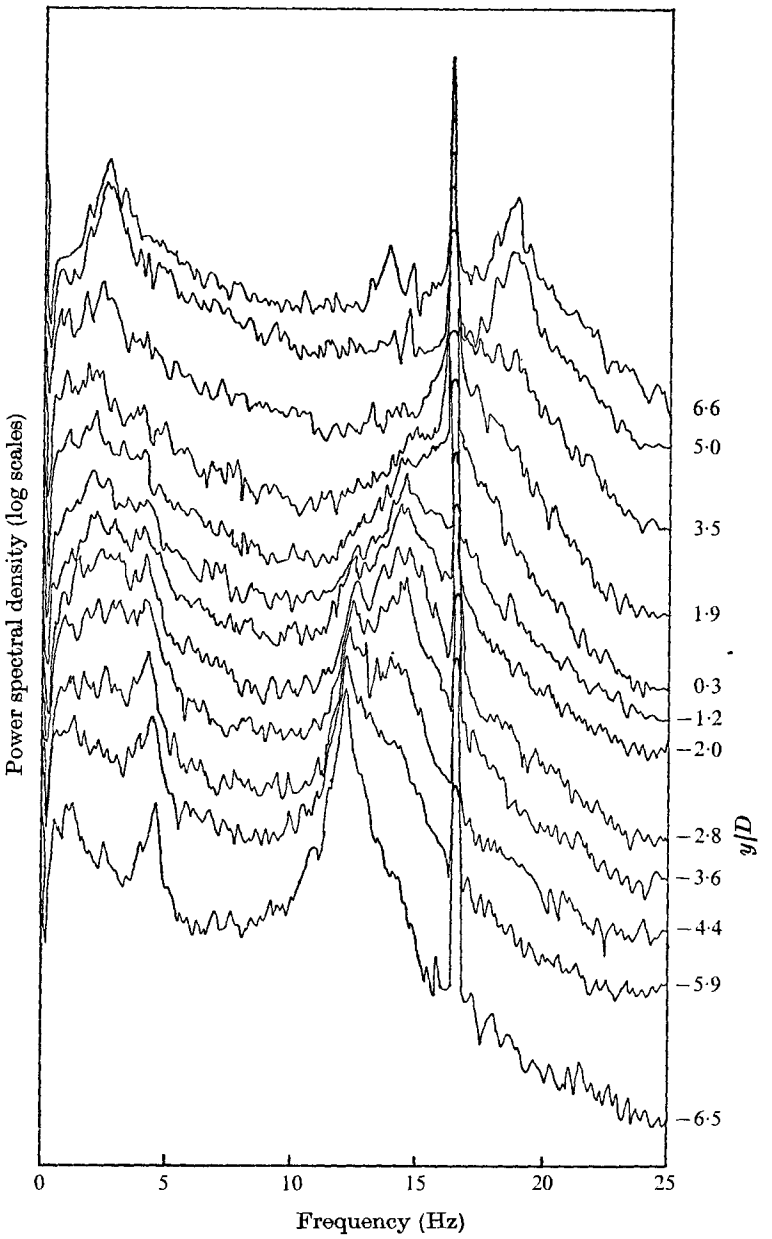

FIGURE 12. Frequency spectra at various spanwise positions for an oscillating cylinder with $H/D = 16$; $a/D = 0{\cdot}06$ and $S_c = 0{\cdot}198$.

When the cell locked-on at the cylinder frequency extends over only part of the span, ϕ varies in the parts of the span adjacent to the locked-on cell which are not also close to the ends, as well as in the parts of the span where the cell is locked-on (see figure 16 for the 25·4 mm cylinder with $a/D = 0{\cdot}06$ and $S_c = 0{\cdot}198$).

H/D	a/D	S_c	S_s for unforced cells at the boundaries of primary locking-on
16	0·06	0·198	0·229 and 0·173
16	0·06	0·155	0·200 and 0·143
16	0·20	0·174	— and 0·125
16	0·20	0·107	0·160 and —
8	0·10	0·168	0·202 and 0·147

TABLE 3

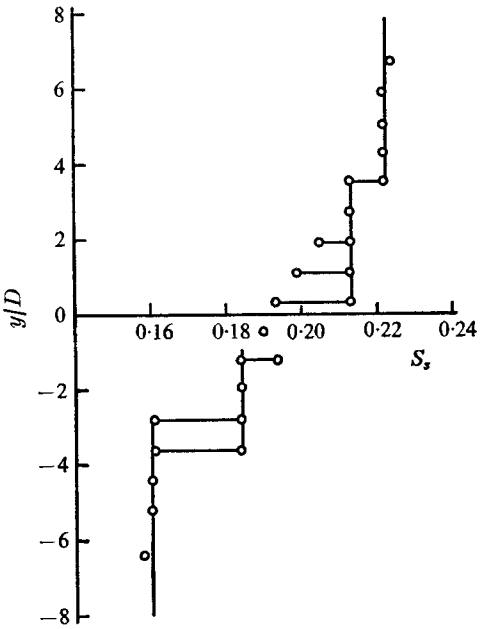

FIGURE 13. Spanwise distribution of S_s with $H/D = 16$, $a/D = 0{\cdot}20$ and $S_c = 0{\cdot}107$.

Further measurements. Measurements were made using two probes to try to determine the mean inclinations of vortices to the cylinder axis. The position of one probe was fixed and the other was moved in a plane parallel to the cylinder axis and the free-stream direction and containing the position of the fixed probe. When the coherence at the shedding frequency is very close to unity the position of the moving probe, when its signal is in phase with that of the fixed probe, can be accurately determined. For $H/D = 16$, with $a/D = 0{\cdot}20$ and $S_c = 0{\cdot}167$, the shedding is completely locked-on across the whole span and such probe positions, as well as the positions of the fixed probe, are shown in figure 17 for two different positions of the fixed probe.

5.2. *The interpretation of spanwise variation in* ϕ

When shedding is not locked-on, the cylinder oscillation will cause the wake to assume a roughly sinusoidal form (compare with a cylinder moving at constant velocity in still air or water and oscillating normal to this velocity). There would

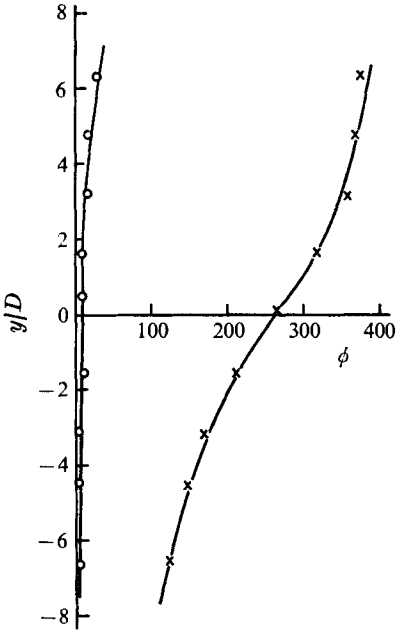

FIGURE 14. Spanwise distributions of ϕ with $H/D = 16$ and $a/D = 0{\cdot}20$. ○, $S_c = 0{\cdot}107$; ×, $S_c = 0{\cdot}167$.

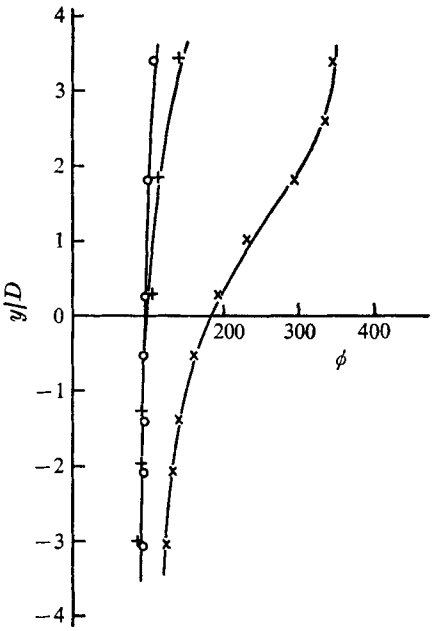

FIGURE 15. Spanwise distributions of ϕ with $H/D = 8$ and $a/D = 0{\cdot}29$. ○, $S_c = 0{\cdot}354$; +, $S_c = 0{\cdot}280$; ×, $S_c = 0{\cdot}168$.

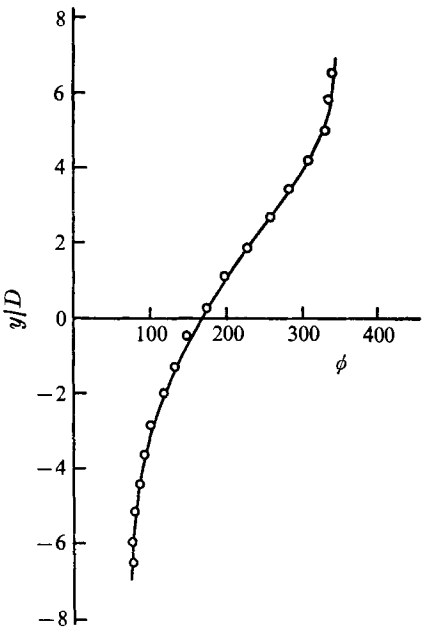

FIGURE 16. Spanwise distributions of ϕ with $H/D = 16$, $a/D = 0{\cdot}06$ and $S_c = 0{\cdot}198$.

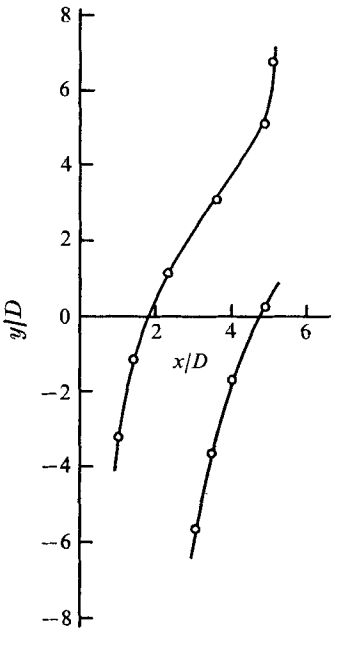

FIGURE 17. Approximate vortex shape as shown by in-phase probe positions for $H/D = 16$, $a/D = 0{\cdot}20$ and $S_c = 0{\cdot}167$.

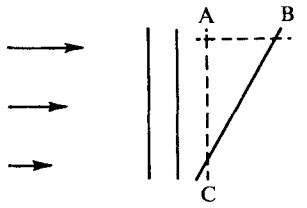

FIGURE 18

be no spanwise variation in ϕ if the wake structure were the same at every spanwise section. This is unlikely to be the case, but as the probe is positioned $1{\cdot}00D$ downstream of and $2{\cdot}15D$ across from the cylinder axis in its mid-position, the part of the body where the flow is attached will define the flow field at the probe to a large extent. Thus it is to be expected that the spanwise variation will be very small.

With locking-on the situation is different. The results of Simmons (1974) (for a D-shaped body) suggest that the convection velocity (or phase speed) could vary by as much as 40 % within one diameter downstream of the probe position but varies very little further downstream. In figure 18, BC represents the shape of the shed vortex and AC the line along which the probe is moved. All points on the line BC will be approximately in phase and the phase difference between A and B or A and C will be given by $\Delta x n_c/kU$, where kU is a representative convection velocity and Δx is the distance between A and B. The in-phase points in figure 17 confirm that vortices locked-on at the cylinder frequency are inclined to the cylinder axis with shapes similar to those in figure 1. Thus spanwise variation of ϕ is indicative of at least primary locking-on but it cannot predict the vortex shape owing to the uncertainty in the streamwise variation of the convection velocity.

5.3. *Discussion*

The spanwise distributions of ϕ are as expected from the considerations of §5.2. When there is no locking-on over any part of the span, ϕ is virtually constant across the span, and when there is primary locking-on ϕ varies over the corresponding part of the span. The very small spanwise variations in ϕ close to the ends in the latter situation are consistent with a vortex approaching an end boundary normally. This is presumably also why there is little spanwise variation in ϕ where the end cells are locked-on at a half and a third of the cylinder frequency with $H/D = 8$. As ϕ varies in parts of the span (away from the ends) where there are also unforced cells, locked-on and unforced shedding must be occurring intermittently, e.g. with $a/D = 0{\cdot}06$ and $S_c = 0{\cdot}198$ ($H/D = 18$). This corresponds to the boundary zones of intermittent primary locking-on in uniform flow.

When shedding is not locked-on at the cylinder frequency, intermittency between two or more different types of shedding can be directly deduced from the spanwise distribution of S_s. These show that shedding is not intermittently locked-on at submultiples of the cylinder frequency, which is consistent with there being no boundary zones in uniform flow. Of necessity, these experiments

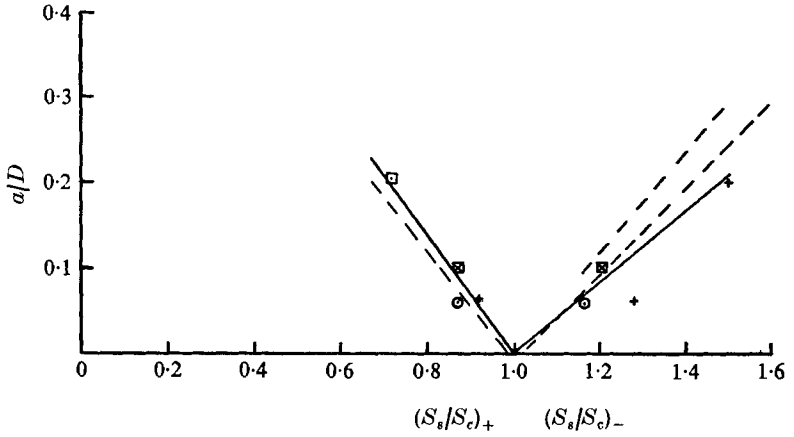

FIGURE 19. The ratios S_s/S_c for the unforced cells at the boundaries of primary locking-on in shear flow for different a/D. ———, uniform flow results of figure 7; ⊠, $S_c = 0{\cdot}168$, $H/D = 8, R_M = 9100$. $H/D = 16, R_M = 3700$: ○, $S_c = 0{\cdot}198$; +, $S_c = 0{\cdot}155$; □, $S_c = 0{\cdot}174$; ×, $S_c = 0{\cdot}107$.

Equations for uniform flow results

$$S_s/S_c = \begin{cases} 1{\cdot}02(1+2{\cdot}00a/D) & \text{for } Re \approx 3600, \\ 1{\cdot}00(1+1{\cdot}69a/D) & \text{for } Re \approx 9200, \\ 0{\cdot}99(1-1{\cdot}60a/D) & \text{for } Re \approx 3600, 9200. \end{cases}$$

were made with $H/D = 8$, and while the lower end cells are locked-on with $a/D = 0{\cdot}29$ for both $S_c = 0{\cdot}280$ and $0{\cdot}354$, the upper unforced end cells had $S_s = 0{\cdot}18$, the corresponding value of S_s for the stationary cylinder being $0{\cdot}204$. This is again consistent with uniform flow results, which showed that, for S_c/S_0 above the range of primary locking-on, unforced shedding frequencies are smaller than the shedding frequency from the stationary cylinder by an amount which increases with increasing a/D. However, results with $H/D = 8$ are not representative of normal cell structure in a shear flow of large spanwise extent and should be regarded with some reserve.

The intermittency between unforced vortex shedding and primary locking-on at the spanwise boundaries of complete locking-on is now established. Boundary zones in uniform flow are characterized by the unforced shedding frequency being directly proportional to the cylinder frequency for different S_c/S_0. This means that the unforced shedding frequencies are being forced away from the values just outside the zones, which are independent of cylinder frequency. In shear flow the values of S_s for unforced cells, which are known to be intermittent with locked-on cells, are also forced away from the values found when the cylinder is stationary. Values of S_s at the boundaries of locking-on were listed in table 3 with corresponding values of S_c and a/D. $(S_s/S_c)_+$ and $(S_s/S_c)_-$ are plotted as functions of a/D in figure 19, where the uniform flow results of figure 7 are shown by the dashed lines. The suffix minus corresponds to the boundary at the high velocity end of locking-on in shear flow and to the lower boundary of locking-on in uniform flow; the suffix plus corresponds to the low velocity end of locking-on in shear flow and to the upper boundary of locking-on in uniform flow. Figure 19

shows there to be some quantitative correspondence between the boundary situations in uniform and shear flows.

In the middle of the range of locking-on in uniform flow there is a jump in the magnitude of ϕ at a certain value of S_c/S_0, but in shear flow there is no such jump at any spanwise position. However, figure 17 indicates that even a locked-on vortex is inclined to the cylinder axis and its movement downstream means that its point of detachment from the cylinder boundary layer is moving down the span. As a result of this, the wake width d' must vary across the span of a locked-on cell. In uniform flow it is proposed that

$$\left(\frac{S_s}{S_c}\right)_+ = \left(\frac{d'_1}{d'_0}\right)_+, \quad \left(\frac{S_s}{S_c}\right)_- = \left(\frac{d'_1}{d'_0}\right)_-.$$

Thus in shear flow the wake width decreases from the high-velocity cell boundary to the low-velocity cell boundary and this change is in sympathy with the necessary change due to the inclination of a vortex to the cylinder axis.

However, it is also possible to consider the situation in a purely geometrical way. If the vortices close to the body are inclined at an angle θ to the cylinder axis, then, as the time taken for d' to change from d'_{1-} to d'_{1+} is $(2n_c)^{-1}$, the vortex will have moved downstream in this time a distance $kU/(2n_c)$ (if the mean vortex convection velocity is kU). Thus the point of detachment of the vortex from the cylinder boundary layer will have moved down the span a distance Δy given by

$$\frac{\Delta y}{D} = \frac{k}{2S_c \tan\theta} \frac{U}{U_M}.$$

This suggests that the spanwise extent of locking-on is independent of a/D.

However, for a given length of span, if a/D is too small the difference between the values of S_s at the boundaries of locking-on as shown in figure 19 might be smaller than the range of S_s for the stationary cylinder over the corresponding length of span. As the unforced values of S_s at the boundaries must be forced away from S_c rather than closer to it, then, for locking-on over a given length of span to occur, the difference between the values of S_s at the boundaries must overlap the range of values of S_s for the stationary cylinder. This is thought to be the most important consideration in defining the spanwise extent of locking-on which might be modified by the influence of vortex inclination.

The experimental results show that cylinder oscillation has a stabilizing effect on the frequencies of the unforced cells only when they are intermittent with the locked-on cells. The shedding frequency of an unforced cell is thought to equal $n_c d'_{1u}/d'_{1f}$ (see appendix) and, if $d'_{1u} = d'_0$, this frequency can vary only as d'_{1f} varies. As the segments of span at the boundaries tend to be small, the range of values for d'_{1f} will be small with a correspondingly small range of unforced shedding frequencies, as shown in figure 10 (*a*), for example.

It is now possible to devise a general formula for the spanwise extent of primary locking-on, provided certain simplifying assumptions are made. It was shown by Mair & Stansby (1975) that $S = n_s D/U$ (where $U = U_M + \lambda y$) is nearly

constant for spanwise positions over a central part of the span when H/D is greater than about 20. If S is constant, as

$$n_s D/U = S,$$

$$S_s = S\left(1+\frac{y}{U_M}\frac{dU}{dy}\right) = S\left(1+\frac{y}{D}\beta_M\right).$$

If the upper limit of locking-on occurs at $y = y_2$ and the lower limit occurs at $y = y_1$, then (from figure 19)

$$S_c(1+\alpha_1 a/D) = S(1+(y_2/D)\beta_M)$$

and

$$S_c(1-\alpha_2 a/D) = S(1+(y_1/D)\beta_M),$$

where α_1 and α_2 are empirical constants. Therefore $(y_2-y_1)/D$ or

$$\Delta y/D = (a/D)(\alpha_1+\alpha_2)\beta_M^{-1} S_c/S.$$

As a limit of locking-on is never a point but always a region of span, the above formula is necessarily an approximation. Also no account is taken of the effect of vortex inclination and of the effect a/D has on the unforced shedding frequencies. The value of $\alpha_1+\alpha_2$ is calculated from the data in figure 19 to be about 4·0.

In the present experiments β_M could be varied only by decreasing H/D below 16. Two values of β_M were used: 0·025 with $H/D = 16$ and 0·050 with $H/D = 8$. For the latter the cell structure is far from that idealized above. Nevertheless, for primary locking-on across the whole span, doubling β_M halved $\Delta y/D$ with only slightly different a/D and S_c, in approximate accordance with the above formula. Further experiments with large H/D (preferably greater than 30) are necessary to investigate the relationship further.

6. Conclusions

Secondary and tertiary locking-on as well as primary locking-on can occur in both uniform and shear flows. In uniform flow primary and tertiary locking-on occur for a range of cylinder frequencies dependent on a/D and Reynolds number; secondary locking-on occurs only over a very small range of cylinder frequencies.

In uniform flow, the boundaries of primary locking-on are characterized by intermittent locking-on. Consideration of this allied to consideration of the universal Strouhal number shows how the wake width is influenced by locking-on. It is conjectured that the wake width jumps at a particular cylinder frequency near the middle of the locked-on range from being greater than to being less than that for the stationary cylinder.

In the shear flow the spanwise extent of primary locking-on is explained by the uniform flow results, taking into account the inclination of locked-on vortices in shear flow. Again locking-on is intermittent at the boundaries. For the Reynolds numbers of these experiments, the spanwise extent of this locking-on is approximately predicted by the following formula:

$$\frac{\Delta y}{D} = \frac{a}{D}\frac{4{\cdot}0}{\beta_M}\frac{S_c}{S}.$$

This work was carried out at the Engineering Department of the University of Cambridge and the author is grateful to Professor W. A. Mair for much helpful criticism and advice. The author was in receipt of a Science Research Council award while undertaking this work.

Appendix

The conventional Strouhal number S for a stationary cylinder in a stream is defined as $n_{s0}d/U$, where d is the cylinder base width. In an attempt to produce a Strouhal number independent of cylinder shape, Roshko (1954) defined a Strouhal number $S' = n_{s0}d'/U'$, where $\beta = U'/U = (1-C_{pb})^{\frac{1}{2}}$; C_{pb} is the base pressure coefficient and d' is the wake width, which can be determined by Roshko's notched hodograph theory. In this way d' is defined by β for a given cylinder shape. Roshko also defined a Reynolds number $Re' = U'd'/\nu$ and suggested that S' should depend only on Re'. In fact Roshko's results showed that S' was nearly constant for Re' between 10^4 and $4{\cdot}4 \times 10^4$.

A similar universal Strouhal number can also be defined for the vortex wakes produced by oscillating cylinders. If the suffix 0 applies to the cylinder when stationary and the suffix 1 to the cylinder when oscillating, then

$$S'_0 = n_{s0}d'_0/\beta_0 U, \quad S'_1 = n_s d'_1/\beta_1 U.$$

At the boundaries of locking-on at the cylinder frequency, where the shedding is intermittently locked-on and unforced at a given cylinder frequency, if S'_1 is always the same, then

$$(n_s d'_1/\beta_1 U)_u = (n_c d'_1/\beta_1 U)_f,$$

where the subscripts u and f stand for 'unforced' and 'locked-on' respectively, and

$$\frac{n_s}{n_c} = \frac{\beta_{1u}}{\beta_{1f}} \frac{d'_{1f}}{d'_{1u}}.$$

As the base pressure is likely to be the same whether the shedding is locked-on or not,

$$n_s/n_c = d'_{1f}/d'_{1u}.$$

REFERENCES

Bishop, R. E. D. & Hassan, A. Y. 1964 *Proc. Roy. Soc.* A **277**, 51.

Elder, J. W. 1959 *J. Fluid Mech.* **5**, 355.

Linke, W. 1931 *Phys. Z.* **32**, 900.

Mair, W. A. & Stansby, P. K. 1975 *SIAM J. Appl. Math.* **28**, 519.

Maskell, E. C. 1965 *Aero. Res. Counc. R. & M.* no. 3400.

Maull, D. J. 1969 *AGARD Conf. Proc.* no. 48, paper 16.

Maull, D. J. & Young, R. A. 1973 *J. Fluid Mech.* **60**, 401.

Owen, P. R. & Zienkiewicz, K. H. 1957 *J. Fluid Mech.* **2**, 521.

Roshko, A. 1954 *N.A.C.A. Tech. Note*, nos. 3168, 3169.

Simmons, J. E. L. 1974 *J. Fluid Mech.* **64**, 599.

Stansby, P. K. 1974 *Aero. J.* **78**, no. 757.